Synthesis, Structure, and Reactivity of Paramagnetic Iron(II) and Iron(III) Amidodiphosphine Complexes

Michael D. Fryzuk,* Daniel B. Leznoff, Erin S. F. Ma, Steven J. Rettig,† and Victor G. Young, Jr.‡

Department of Chemistry, University of British Columbia, 2036 Main Mall, Vancouver, British Columbia, Canada V6T 1Z1

Received August 1, 1997

The preparation and characterization of a series of divalent and trivalent iron complexes that incorporate the amidodiphosphine ligand $N(SiMe_2CH_2PPh_2)_2$ are reported. Mononuclear, tetrahedral complexes of the type $FeX[N(SiMe_2CH_2PPh_2)_2]$, where X = Cl, Br, have been prepared; magnetic susceptibility studies indicate that these are high-spin d^6 systems. The preparation of Fe(II) alkyls of the formula $FeR[N(SiMe_2CH_2PPh_2)_2]$ was examined; small alkyl substituents such as R = Me or CH_2Ph were found to be thermally unstable and, thus, not isolable; however, for R = CH_2SiMe_3 and $CH(SiMe_3)_2$, room-temperature stable, yellow, paramagnetic solids could be obtained. The reaction of $FeCl[N(SiMe_2CH_2PPh_2)_2]$ with NaCp•-DME generates the thermally stable, diamagnetic complex $Fe(\eta^5\text{-}C_5H_5)[N(SiMe_2CH_2PPh_2)_2]$. The corresponding Fe(III) derivative $FeX_2[N(SiMe_2CH_2PPh_2)_2]$ could be prepared in high yield by direct reaction of the $LiN(SiMe_2CH_2PPh_2)_2$ ligand precursor with either $FeCl_3$ or $FeBr_3$. Variable-temperature magnetic susceptibility studies indicate that $FeBr_2[N(SiMe_2CH_2PPh_2)_2]$ is an example of a spin-admixed system ($S = {}^3/_2$ and ${}^5/_2$ spin states).

Introduction

The organometallic chemistry of iron is dominated by complexes that contain cyclopentadienyl and/or carbonyl ligands.[1,2] Such complexes have found widespread use in organic synthesis and have also helped delineate fundamental processes in organometallic chemistry. In an effort to expand organoiron chemistry, we have examined the synthesis and reactivity of Fe(II) and Fe(III) complexes stabilized by the mixed-donor multidentate ligand $N(SiMe_2CH_2PPh_2)_2$. Our original design strategy was to take advantage of the fact that this potentially tridentate ligand should be able to stabilize metal complexes in variable oxidation states due to the presence of the vastly different donor types;[3−5] the amide portion of the ligand can stabilize metals in high valency states, while the phosphine donors are known to stabilize low oxidation states. Using this ligand system, we have been able to prepare complexes in which the central metal is in an unusual oxidation state, for example, mononuclear Zr(III) and Hf(III) derivatives,[6] and study changes in oxidation states, most recently with Co(II) and Co(III) by reaction with alkyl halides.[7] Thus, the extension to Fe(II) and Fe(III) seemed logical.

In this paper we report the synthesis of divalent iron complexes of the formula $FeX[N(SiMe_2CH_2PPh_2)_2]$. These Fe(II) derivatives serve as useful precursors to the formation of thermally labile, paramagnetic alkyl derivatives.[1,8] Complexes that contain Fe(II) and Fe(III) can show a wide range of magnetic behavior;[9] in this work, we detail the structure and variable-temperature magnetic susceptibility studies of an unusual, spin-admixed Fe(III) complex.

Results and Discussion

Synthesis and Reactivity of Iron(II) Halide Complexes. Dropwise addition of the lithium salt $LiN(SiMe_2CH_2PPh_2)_2$ to a slurry of FeX_2 (X = Cl, Br) in THF (eq 1) gives the toluene-soluble complexes $FeX[N(SiMe_2CH_2PPh_2)_2]$ (X = Cl (**1**), Br (**2**)) as slightly beige powders in high yield. The complexes have a solution magnetic

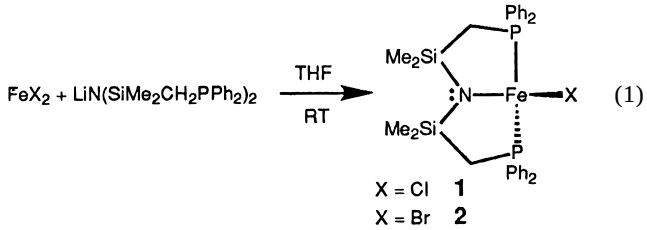

(1)

moment[10,11] of 4.9 μ_B, consistent with a high-spin d^6

† Professional Officer: UBC X-ray Structural Laboratory.
‡ X-ray Crystallographic Center, Department of Chemistry, 160 Kolthoff Hall, University of Minnesota, Minneapolis, MN 55455.

(1) von Gustorf, E. A. K.; Grevels, F. W.; Fischer, I. *The Organic Chemistry of Iron*; Academic: London, 1978; Vol. I.
(2) Pearson, A. J. *Metallo-organic Chemistry*; Wiley: New York, 1985; Chapters 7 and 8.
(3) Fryzuk, M. D.; Montgomery, C. D. *Coord. Chem. Rev.* **1989**, *95*, 1.
(4) Fryzuk, M. D.; Berg, D. J.; Haddad, T. S. *Coord. Chem. Rev.* **1990**, *99*, 137.
(5) Fryzuk, M. D. *Can. J. Chem.* **1992**, *70*, 2839.
(6) Fryzuk, M. D.; Mylvaganam, M.; Zaworotko, M. J.; MacGillivray, L. R. *Polyhedron* **1996**, *15*, 689.
(7) Fryzuk, M. D.; Leznoff, D. B.; Thompson, R. C.; Rettig, S. J.; Young, V. G., Jr.; Yap, G. P. **1998**, submitted for publication.
(8) Poli, R. *Chem. Rev.* **1996**, *96*, 2135.
(9) Kahn, O. *Molecular Magnetism*; VCH: New York, 1993.
(10) Evans, D. F. *J. Chem. Soc.* **1959**, 2003.

S0276-7333(97)00665-1 CCC: $15.00
Publication on Web 05/08/1998

system (four unpaired electrons).[12] FeX[N($SiMe_2CH_2PPh_2$)$_2$] is ESR-silent, but broad peaks are visible in the ^{1}H NMR spectra. Unfortunately, it is difficult to assign the spectrum due to extreme broadness (leading to unreliable integration) and missing peaks. Knowledge of the spectra, however, is useful in compound identification.

Despite extensive efforts, X-ray-quality crystals of the halide complexes could not be obtained. However, on the basis of the spectroscopic evidence, halides **1** and **2** are likely mononuclear and tetrahedral. The measurement of a high-spin d^6 system rules out the possibility of square-planar coordination as square-planar iron(II) complexes such as Fe(C_6Cl_5)$_2$(PEt_2Ph)$_2$ are generally low spin.[13] A dimeric species can be excluded as it would be expected to show lower solubility in toluene, as found for the related chromium(II) chloride dimer {[($Ph_2PCH_2SiMe_2$)$_2$N]Cr}$_2$(μ-Cl)$_2$. Other tetrahedral iron(II) phosphine halide complexes are known and include $FeCl_2$(dippe),[14] $FeCl_2(PEt_nPh_{3-n})_2$,[15] $FeCl_2$(depe),[16] and FeX_2(dppe).[17,18] A tetrahedral, structurally characterized Fe(II) amide FeCl[NR′Ar_f](TMEDA) (R′ = $C(CD_3)_2CH_3$, $C(CD_3)_2Ph$; Ar_f = 2,5-C_6H_3FMe)[19] and several Fe(II) thiolates[20] and selenolates[21,22] have also been reported. All of these examples are high-spin Fe(II) compounds, with magnetic moments ranging from 4.8 to 5.3 μ_B.

Addition of weak donor solvents such as acetonitrile or THF to iron chloride **1** caused no change in the UV−vis spectrum. Addition of 1 atm of CO to a toluene solution of **1** also yielded no obvious spectral changes. Only upon addition of pyridine, a strong σ-donor, was an effect observable. This is in stark contrast to the reactions of the chromium chloride dimer {[($Ph_2PCH_2SiMe_2$)$_2$N]Cr}$_2$(μ-Cl)$_2$ with donor ligands, which generate five-coordinate adducts even with weak donors.[23,24]

The ligation of pyridine to **1** can be monitored by UV−vis spectroscopy due to the growth of a band at 370 nm upon addition of pyridine. Further addition caused a shift of this band to 388 nm; hence, a two-step equilibrium involving a mono(pyridine) adduct and a bis(pyridine) derivative is proposed (eqs 2 and 3).

$$\mathrm{FeCl[N(SiMe_2CH_2PPh_2)_2]} + \mathrm{py} \overset{K_1}{\rightleftharpoons} \mathrm{FeCl(py)[N(SiMe_2CH_2PPh_2)_2]} \quad (2)$$

$$\mathrm{FeCl(py)[N(SiMe_2CH_2PPh_2)_2]} + \mathrm{py} \overset{K_2}{\rightleftharpoons} \mathrm{FeCl(py)_2[N(SiMe_2CH_2PPh_2)_2]} \quad (3)$$

Scheme 1

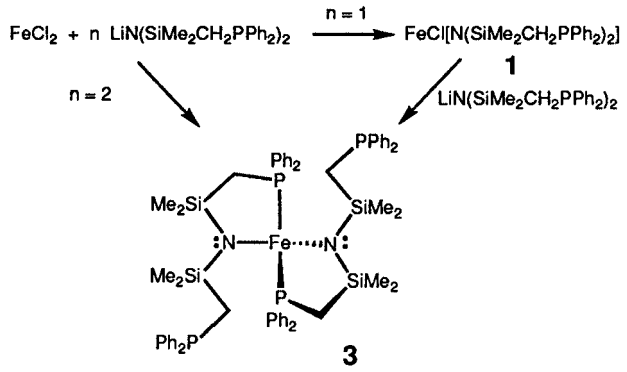

These pyridine complexes are deep orange but could not be isolated for elemental analysis, even from neat pyridine. However, careful titration with stoichiometric and then excess pyridine yielded equilibrium constants for ligation of one and then two pyridines to the tetrahedral iron center. Analysis of the above data gave order-of-magnitude estimates of $K_1 = 2 \times 10^4$ and $K_2 = 6$.

Although it is tempting to definitively assign the mono- and bis(pyridine) adducts as five- and six-coordinate species, respectively, the evidence is inconclusive. In particular, the solution magnetic moment of **1** in pyridine-d_5 is 4.9 μ_B, implying that tetrahedral coordination is preserved (octahedral, high-spin Fe(II) generally has a higher μ_{eff} than tetrahedral Fe(II) due to a first-order orbital contribution). However, the ^{1}H NMR spectrum of chloride **1** in pyridine-d_5 shows no substantial change from that observed in benzene-d_6; one would expect shifted resonances (versus uncomplexed **1**) due to the fluxionality of the phosphine arms if tetrahedral coordination was preserved. Finally, the ^{31}P{^{1}H} NMR spectrum of chloride **1** in pyridine-d_5 is barren of peaks, implying that the phosphines are bound to the paramagnetic Fe(II) center at least some of the time.

Synthesis and Structure of a Bis(ligand) Iron(II) Complex. In the preparation of chloride **1** (eq 1), a capricious side product was formed in low yields. However, because this material formed X-ray-quality crystals, we were able to determine its structure. Pale green crystals were obtained and shown to be the bis(ligand) complex Fe[N($SiMe_2CH_2PPh_2$)$_2$]$_2$ (**3**); the molecular formula was confirmed by an elemental analysis on material synthesized in good yield by the appropriate stoichiometry changes as outlined in Scheme 1. Such bis(ligand) complexes of the general formula M[N($SiMe_2CH_2PPh_2$)$_2$]$_2$ (M = Cr, Co) have been previously suggested to lower the yields of the mono(ligand) derivatives MX[N($SiMe_2CH_2PPh_2$)$_2$].[23,24]

A solution magnetic moment of 4.7 μ_B for **3** was measured by Evans' method and is consistent with a high-spin d^6 tetrahedral system. The mass spectrum shows a molecular ion peak at 1112 *m/e*, loss of a CH_2PPh_2 arm at 913 *m/e*, and the base peak M^+ − [N($SiMe_2CH_2PPh_2$)$_2$] at 584 *m/e*. There are no signals assignable to chloride-containing species in the spectrum, consis-

(11) Sur, S. K. *J. Magn. Reson.* **1989**, *82*, 169.
(12) Carlin, R. L. *Magnetochemistry*; Springer-Verlag: Heidelberg, 1986.
(13) Chatt, J.; Shaw, B. L. *J. Chem. Soc.* **1961**, 185.
(14) Hermes, A. R.; Girolami, G. S. *Inorg. Chem.* **1988**, *27*, 1775.
(15) Booth, G.; Chatt, J. *J. Chem. Soc.* **1962**, 2099.
(16) Henderson, R. A. *J. Chem. Soc., Dalton Trans.* **1988**, 509.
(17) Hata, G.; Kondo, H.; Miyake, A. *J. Am. Chem. Soc.* **1968**, *90*, 2278.
(18) Baker, W. A.; Lutz, P. M. *Inorg. Chim. Acta* **1976**, *16*, 5.
(19) Stokes, S. L.; Davis, W. M.; Odom, A. L.; Cummins, C. C. *Organometallics* **1996**, *15*, 4521.
(20) Bierbach, U.; Saak, W.; Haase, D.; Pohl, S. *Z. Naturforsch. B* **1991**, *46*, 1629.
(21) Forde, C. E.; Morris, R. H.; Ramachandran, R. *Inorg. Chem.* **1994**, *33*, 5647.
(22) McConnachie, J. M.; Ibers, J. A. *Inorg. Chem.* **1991**, *30*, 1770.
(23) Fryzuk, M. D.; Leznoff, D. B.; Rettig, S. J.; Thompson, R. C. *Inorg. Chem.* **1994**, *33*, 5528.
(24) Fryzuk, M. D.; Leznoff, D. B.; Rettig, S. J. *Organometallics* **1995**, *14*, 5193.

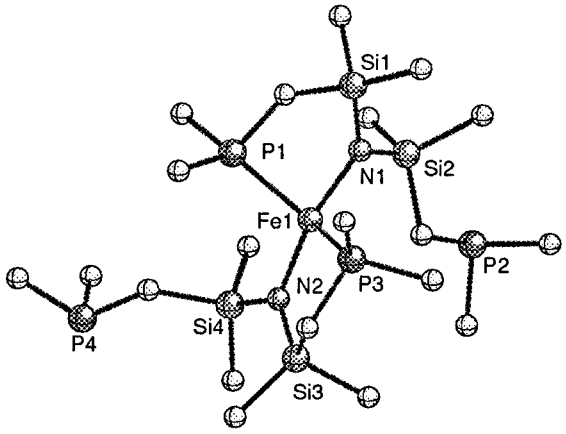

Figure 1. Molecular structure (ball and stick) and numbering scheme for $Fe[N(SiMe_2CH_2PPh_2)_2]_2$ (3). Only the phenyl ipso carbons on phosphorus are included for clarity.

Scheme 2

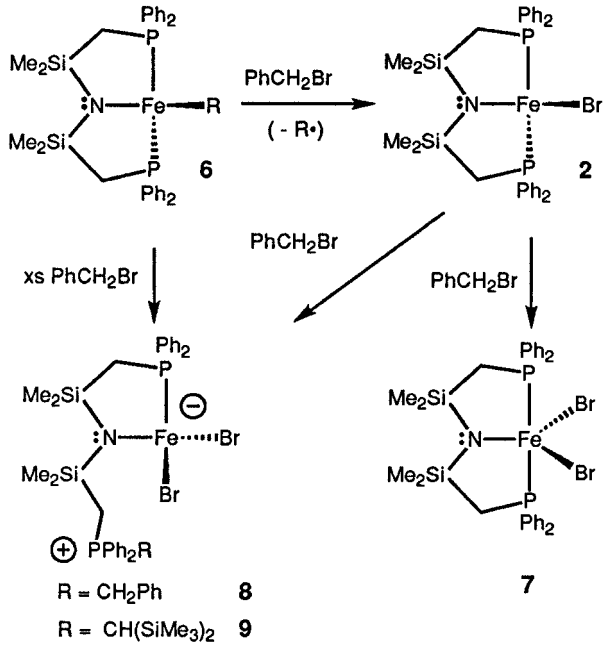

tent with the bis(ligand) formulation. The ^1H NMR spectrum for bis(ligand) complex **3** contains four broad peaks which can be tentatively assigned using integration and relative broadness to ligand backbone peaks; the backbone methylene CH_2 peaks are too broad to be observed. The unique $SiMe_2$ resonance appears at +20.5 ppm, the meta proton resonance at +10.8 ppm, and the ortho and para resonances at +1.0 and −1.0 ppm, respectively. The observation of only one set of resonances for the ligand implies a fluxional process in action that makes the two sides of the chelate arm equivalent. The $^{31}P\{^1H\}$ NMR spectrum of **3** is devoid of peaks, a fact that can also be attributed to a fluxional process involving dissociation and reassociation of the chelating phosphines to the paramagnetic center.

The crystal structure, shown in Figure 1, reveals the tetrahedral coordination around the iron center, with each potentially tridentate ligand bound through the central amide and one phosphine, that is, in a bidentate fashion. Crystallographic data for all structures reported are in Table 1; selected bond lengths and angles for **3** are found in Table 2. The complex probably remains tetrahedral due to the steric congestion around the metal. The distortions in the tetrahedral array manifest themselves in the coordination-sphere bond angles, which range from 90.97(7)° (P(1)−Fe−N(1)) to 142.50(9)° (N(1)−Fe−N(2)).

Typical octahedral low-spin Fe(II)−P bonds range from 2.24 to 2.30 Å, while octahedral high-spin complexes have Fe−P bonds which are much longer, typically from 2.58 to 2.68 Å.[25] The Fe−P bond lengths of 2.4580(7) and 2.4696(7) Å in the bis(ligand) complex **3** are intermediate between these two extremes. These Fe−P bond lengths compare well with other tetrahedral iron(II)−P bond lengths such as 2.426(1) Å in $Fe(Se\text{-}2,6\text{-}^iPr_2\text{-}C_6H_3)_2(PMe_2Ph)_2$,[21] 2.408(2) and 2.447(2) Å in $Fe(Se\text{-}2,6\text{-}^iPr_2\text{-}C_6H_3)_2(depe)$,[21] and 2.47(1) Å in $FeCl_2$(dippe).[14]

There are a number of iron(II) amide complexes with low coordination numbers that have been structurally characterized. Some examples include $Fe[N(SiMePh_2)_2]_2$,[26] $Fe[N(SiMe_3)_2]_2(THF)$,[27] and FeCl(TMEDA)[NR′Ar_f] (R′ = $C(CD_3)_2CH_3$, $C(CD_3)_2Ph$; Ar_f = 2,5-C_6H_3FMe),[19] with Fe−N bond lengths of 1.917(2), 1.927(3), and 1.916(5) and 1.918(3) Å, respectively. The corresponding Fe−N distances in the bis(ligand) complex **3** of 1.981(2) and 1.987(2) Å are slightly longer than those observed in other iron(II) amides, presumably due to steric crowding. The N−Si bond lengths in **3** range from 1.712(2) to 1.725(2) Å and are comparable to those observed in the iron(II) amides in $Fe[N(SiMe_3)_2]_2(THF)$[27] (1.709(5) Å) and $Fe[N(SiMe_3)_2]_2$ (1.723(5) Å, gas-phase electron diffraction).[28]

Synthesis and Structure of $Fe(\eta^5\text{-}C_5H_5)[N(SiMe_2CH_2PPh_2)_2]$ (4). Dropwise addition of a solution of NaC_5H_5·DME (DME = 1,2-dimethoxyethane) to a THF solution of chloride **1** at −78 °C caused a color change to dark red, and from the resulting solution red crystals of $Fe(\eta^5\text{-}C_5H_5)[N(SiMe_2CH_2PPh_2)_2]$ (**4**) were isolated and characterized (eq 4). This complex is analogous to those

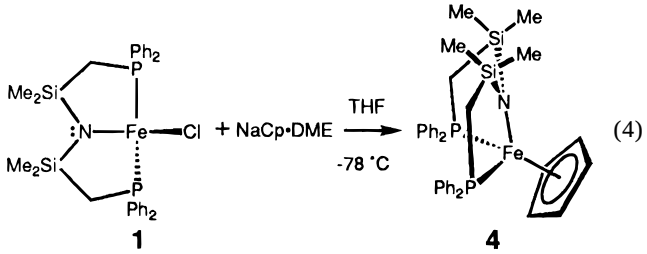

(4)

prepared with chromium and cobalt metal centers.[7,23,24]

The X-ray crystal structure (Figure 2) of the 18-electron, diamagnetic $Fe(\eta^5\text{-}C_5H_5)[N(SiMe_2CH_2PPh_2)_2]$ (**4**) revealed the expected monomeric distorted pseudo-octahedral geometry. The bond angles (Table 3) around the iron center of 123.2°, 124.1°, and 124.0° (P(1)−Fe−Cp, P(2)−Fe−Cp, and N−Fe−Cp) are comparable to those found in the chromium analogue.[24] The Fe−P bond lengths (Table 3) of 2.256(1) and 2.242(1) Å are

(25) DiVaira, M.; Midollini, S.; Sacconi, L. *Inorg. Chem.* **1981**, *20*, 3430.
(26) Bartlett, R. A.; Power, P. P. *J. Am. Chem. Soc.* **1987**, *109*, 7563−7564.
(27) Olmstead, M. M.; Power, P. P.; Shoner, S. C. *Inorg. Chem.* **1991**, *30*, 2547.
(28) Andersen, R. A.; Faegri, K., Jr.; Green, J. C.; Haaland, A.; Lappert, M. F.; Leung, W. P.; Rypdal, K. *Inorg. Chem.* **1988**, *27*, 1782.

Table 1. Crystallographic Data

compound	**3**[a]	**4**[b]	**6**[a]	**7**[a]
formula	$C_{60}H_{72}FeN_2P_4Si_4$	$C_{35}H_{41}FeNP_2Si_2$	$C_{37}H_{55}FeNP_2Si_4$	$C_{33}H_{39}Br_2FeNP_2Si_2$
fw	1113.29	649.68	743.97	783.44
color, habit	brown, block	red, prism	colorless, irregular	brown, block
cryst size, mm	0.50 × 0.25 × 0.12	0.20 × 0.30 × 0.40	0.50 × 0.18 × 0.04	0.26 × 0.08 × 0.05
cryst syst	orthorhombic	monoclinic	monoclinic	triclinic
space group	$Pca2_1$	$P2_1/n$ (No. 14)	$P2_1/n$ (No. 14)	$P\bar{1}$ (No. 2)
a, Å	15.7747(3)	15.842(2)	11.3293(1)	9.8961(2)
b, Å	18.7736(3)	12.532(3)	16.6607(2)	11.6989(3)
c, Å	20.5858(4)	17.803(2)	22.3181(3)	16.1366(4)
α, deg	90	90	90	97.767(1)
β, deg	90	111.144(8)	99.048(1)	91.290(1)
γ, deg	90	90	90	97.852(1)
V, Å^3	6096.4(2)	3295.9(9)	4160.21(8)	1832.10(8)
Z	4	4	4	2
T, °C	−100	21	−100	−100
ρ_{calc}, g/cm^3	1.213	1.309	1.188	1.420
F(000)	2352	1368	1584	796
radiation	Mo	Mo	Mo	Mo
μ, cm^{-1}		6.52		
transmission factors	0.79−0.95	0.94−1.00	0.849−1.00	0.523−1.00
scan type		$\omega-2\theta$		
scan range, deg in ω		1.26 + 0.35 tan θ		
scan speed, deg/min		16 (up to 8 rescans)		
data collected	$\pm h, \pm k, \pm l$	$+h, \pm k, \pm l$	$\pm h, +k, +l$	$\pm h, \pm k, +l$
$2\theta_{max}$, deg	50	55	50	50
crystal decay, %	negligible	negligible	negligible	negligible
total no. of reflns	29 157	8212	20 694	10 443
no. of unique reflections	9622	7926	7254	6135
R_{merge}	0.0281	0.031	0.0274	0.0448
no. with $I \geq n\sigma(I)$	9620	3882	7254	6125
no. of variables	720	371	471	401
R	0.0285	0.037	0.0317	0.0704
R_w	0.0337	0.037	0.0433	0.1107
gof	1.060	1.80	1.019	0.981
max Δ/σ		0.0004		
residual density e/Å^3	−0.159, 0.218	−0.21, 0.60	−0.24, 0.241	−1.887, 1.196

[a] Siemens SMART CCD diffractometer, function minimized $\sum w(|F_o| - |F_c|)^2$, where $w^{-1} = \sigma^2(F_o) + 0.0010F_o^2$, $R = \sum||F_o| - |F_c||/\sum|F_o|$, $R_w = \sum|(w^{1/2}(F_o - F_c)|/\sum|(w)^{1/2}F_o|$, and gof = $[\sum w(|F_o| - |F_c|)^2/(m - n)]^{1/2}$. Values given for R, R_w, and gof are based on those reflections with $I \geq 2\sigma(I)$. [b] Rigaku AFC6S diffractometer, takeoff angle 6.0°, aperature 6.0 × 6.0 mm at a distance of 285 mm from the crystal, stationary background counts at each end of the scan (scan/background time ratio 2:1), Cu Kα (λ = 1.541 78 Å) or Mo Kα radiation (λ = 0.710 69 Å), graphite monochromator, $\sigma^2(F^2) = [S^2(C + 4B)]/L_p^2$ (S = scan speed, C = scan count, B = normalized background count), function minimized $\sum w(|F_o| - |F_c|)^2$ where $w = 4F_o^2/\sigma^2(F_o^2)$ for **4**, $R = \sum||F_o| - |F_c||/\sum|F_o|$, $R_w = (\sum w(|F_o| - |F_c|)^2/\sum w|F_o|^2)^{1/2}$, and gof = $[\sum w(|F_o| - |F_c|)^2/(m - n)]^{1/2}$. Values given for R, R_w, and gof are based on those reflections with $I \geq 3\sigma(I)$.

Table 2. Selected Bond Lengths (Å) and Angles (deg) in Fe[N(SiMe$_2$CH$_2$PPh$_2$)$_2$]$_2$ (3)

Fe(1)−P(1)	2.4580(7)	Fe(1)−P(3)	2.4696(7)
Fe(1)−N(1)	1.981(2)	Fe(1)−N(2)	1.987(2)
N(1)−Si(1)	1.725(2)	N(1)−Si(2)	1.721(2)
N(2)−Si(3)	1.717(2)	N(2)−Si(4)	1.722(2)
N(1)−Fe(1)−N(2)	142.50(9)	P(1)−Fe(1)−N(1)	90.97(7)
P(1)−Fe(1)−N(2)	114.50(6)	P(3)−Fe(1)−N(1)	109.05(6)
P(3)−Fe(1)−N(2)	94.61(6)	P(1)−Fe(1)−P(3)	98.33(3)
Fe(1)−N(1)−Si(1)	116.57(12)	Fe(1)−N(2)−Si(3)	114.71(11)
Si(1)−N(1)−Si(2)	121.77(12)	Si(3)−N(2)−Si(4)	123.38(12)

comparable to other low-spin octahedral iron(II) complexes (2.24−2.30 Å)[25] but much shorter than those observed for the bis(ligand) complex **3**, which contains a high-spin tetrahedral iron(II) center. Also, these bond lengths are substantially shorter than those found in the isostructural chromium complex Cr(η^5-C$_5$H$_5$)-[N(SiMe$_2$CH$_2$PPh$_2$)$_2$], which has Cr−P bond lengths of 2.353(3) and 2.366(3) Å.[24] This shortening is essentially due to the smaller iron(II) center vs the chromium(II) center, which in addition to being further left in the periodic series, still contains two unpaired electrons. The crystal radii for octahedral low-spin Fe(II) and Cr(II) centers are 0.75 and 0.87 Å respectively,[29,30] which almost completely account for the differences observed. Similarly, the Fe−Cp(centroid) distance of 1.71 Å is shorter than the 1.86 Å distance observed in the chromium complex.[24] The Fe−N distance of 2.086(3) Å is comparable to the chromium complex (2.066(7) Å) but longer than in the tetrahedral high-spin iron complex

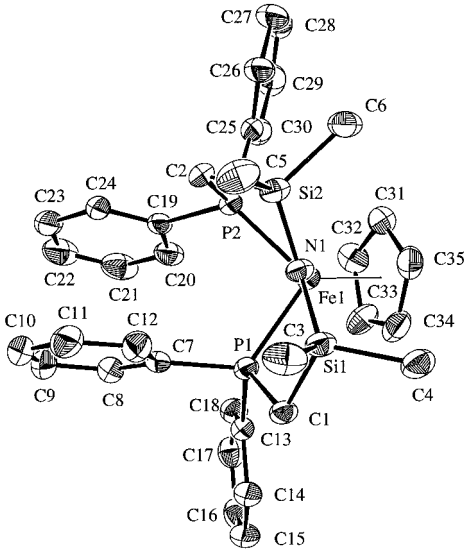

Figure 2. Molecular structure (ORTEP) and numbering scheme for Fe(η^5-C$_5$H$_5$)[N(SiMe$_2$CH$_2$PPh$_2$)$_2$] (4), 33% probability ellipsoids are shown.

(29) Shannon, R. D.; Prewitt, C. T. *Acta Crystallogr. B* **1969**, *B25*, 925.

(30) Shannon, R. D. *Acta Crystallogr. B* **1976**, *A32*, 751.

Table 3. Selected Bond Lengths (Å) and Angles (deg) in Fe(η^5-C_5H_5)[N($SiMe_2CH_2PPh_2$)$_2$] (4)

Fe(1)−P(1)	2.256(1)	Fe(1)−P(2)	2.242(1)
Fe(1)−N(1)	2.086(3)	Fe(1)−C(31)	2.085(4)
Fe(1)−C(32)	2.070(4)	Fe(1)−C(33)	2.077(4)
Fe(1)−C(34)	2.080(4)	Fe(1)−C(35)	2.087(4)
Fe(1)−Cp[a]	1.71	P(1)−C(1)	1.821(3)
Si(1)−N(1)	1.689(3)	Si(2)−N(1)	1.687(3)
C(31)−C(32)	1.403(5)	C(31)−C(35)	1.391(5)
C(32)−C(33)	1.344(5)	C(33)−C(34)	1.397(5)
C(34)−C(35)	1.407(5)		
P(1)−Fe(1)−P(2)	100.14(4)	P(1)−Fe(1)−N(1)	81.73(8)
P(1)−Fe(1)−Cp[a]	125.2	P(2)−Fe(1)−N(1)	89.94(7)
P(2)−Fe(1)−Cp[a]	124.1	N(1)−Fe(1)−Cp[a]	124.0
Fe(1)−N(1)−Si(1)	112.9(1)	Fe(1)−N(1)−Si(2)	111.9(1)
Si(1)−N(1)−Si(2)	135.2(2)		

[a] Cp refers to the unweighted centroid of the C(31−35) ring.

3 by approximately 0.1 Å. Also, the N−Si bond lengths of 1.689(3) and 1.687(3) Å in diamagnetic **4** are considerably shorter than in high-spin **3** (1.720 Å average). These observations could reflect the minimal interaction of the amide lone pair with the metal center in the 18-electron complex **4** (inclusion of the amide lone pair would make this a formally 20-electron species or more appropriately an (18 + δ) complex[31] compared to the 14-electron high-spin **3**.

Synthesis and Characterization of High-Spin Iron(II) Alkyl Complexes. The synthesis of the corresponding iron(II) methyl complex FeMe[N($SiMe_2CH_2PPh_2$)$_2$] was attempted by addition of MeLi to a toluene or THF solution of chloride **1** (eq 5).[7,23,24]

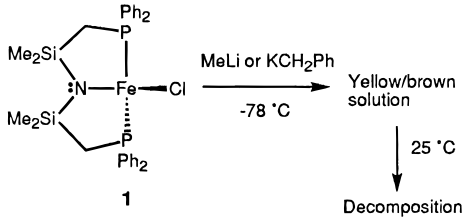

1 (5)

Dropwise addition at −78 °C resulted in a golden brown solution, which turned dark brown upon being warmed to room temperature. Alternately, addition of MeMgBr at −78 °C to **1** resulted in a bright yellow solution, which again changed to dark brown upon being warmed to room temperature. In both cases, removal of the solvent, extraction with hexanes, and filtration through Celite gave an oily brown solid which could not be identified. The mass spectrum did not show any recognizable peaks, and elemental analysis of multiple attempts at this reaction gave irreproducible and unassignable results. Attempted methylation of **1** in the presence of pyridine or phosphine did not result in tractable materials.

An attempt to form a benzyl complex by addition of benzylpotassium in THF at −78 °C to halide **1** gave a bright yellow solution. The appearance of this color was encouraging because it is consistent with many other iron(II) alkyl complexes, for example, Fe(CH_2Ph)$_2$(dippe),[32] FeR_2 (R = $C(SiMe_3)_2C_5H_4N$-2),[33,34] $FePh_2$(PEt_3)$_2$,[35] and Fe(Mes*)$_2$[36,37] are all yellow in color. The yellow color persisted for a few minutes at room temperature, but unfortunately over the course of the workup procedure, decomposition to brown intractable materials occurred.

The observation that the benzyl complex took longer to decompose than the methyl complex implied that steric bulk could be beneficial in the synthesis of iron(II) alkyl derivatives. Sterically demanding hydrocarbyl groups have been used successfully in the synthesis of low-coordinate iron(II) hydrocarbyl complexes. For example, tetrahedral iron(II) dialkyls were prepared in which bulky groups such as CH_2SiMe_3, CH_2CMe_3, and CH_2SiMe_2Ph were used, and in addition, a bis(benzyl) complex was prepared and structurally characterized.[32]

Accordingly, dropwise addition of $LiCH_2SiMe_3$ at −78 °C to a THF solution of **1** gave a bright yellow solution over 10 min which *remained yellow* after standard workup (eq 6). Evaporation of a yellow hexanes solution

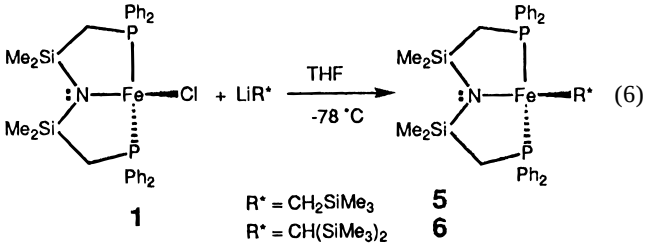

(6)

gave a waxy yellow solid, which gave an elemental analysis consistent with Fe(CH_2SiMe_3)[N($SiMe_2CH_2PPh_2$)$_2$] (**5**). The mass spectrum showed a weak M^+ − Me peak at 663 *m/e* and a strong M^+ − CH_2SiMe_3 peak at 584 *m/e*. The solution magnetic moment (Evans' method)[10,11] of 4.8 μ_B is consistent with a high-spin tetrahedral iron(II) complex. Similarly, reaction of an extremely bulky alkyl, namely $LiCH(SiMe_3)_2$, with chloride **1** produced, after workup, yellow crystals of Fe{$CH(SiMe_3)_2$}[N($SiMe_2CH_2PPh_2$)$_2$] (**6**). The elemental analysis and the solution magnetic moment of 5.3 μ_B confirmed the presence of a high-spin, tetrahedral organoiron(II) complex (four unpaired electrons with a second-order orbital contribution). In this derivative, there was a possibility of an agostic C−H interaction with the metal center but the IR spectrum showed no evidence of this, that is, no C−H stretches below 2850 cm^{-1} were observed.[38] The mass spectrum of the bis(trimethylsilyl)methyl complex **6** was very informative, with many identifiable fragments evident. The molecular ion peak at 743 *m/e* easily lost a proton (likely the alkyl C−H) to yield a cluster at 742 *m/e* (M^+ − H), which overlapped with the molecular ion cluster. Also easily observable was the loss of a methyl group at 728 *m/e* (M^+ − Me), loss of a trimethylsilyl group at 670 *m/e* (M^+

(31) Schut, D. M.; Keana, K. J.; Tyler, D. R.; Rieger, P. H. *J. Am. Chem. Soc.* **1995**, *117*, 8939.
(32) Hermes, A. R.; Girolami, G. S. *Organometallics* **1987**, *6*, 763.
(33) Lee, H. K.; Luo, B. S.; Mak, T. C. W.; Leung, W. P. *J. Organomet. Chem.* **1995**, *489*, C71.
(34) Leung, W. P.; Lee, H. K.; Weng, L. H.; Luo, B. S.; Zhou, Z. Y.; Mak, T. C. W. *Organometallics* **1996**, *15*, 1785.
(35) Maruyama, K.; Ito, T.; Yamamoto, A. *Transition Met. Chem.* **1980**, *5*, 14.
(36) Müller, H.; Seidel, W.; Görls, H. *Angew. Chem., Int. Ed. Engl.* **1995**, *34*, 325.
(37) Wehmschulte, R. J.; Power, P. P. *Organometallics* **1995**, *14*, 3264.
(38) Brookhart, M.; Green, M. L. H.; Wong, L. L. *Prog. Inorg. Chem.* **1988**, *36*, 1.

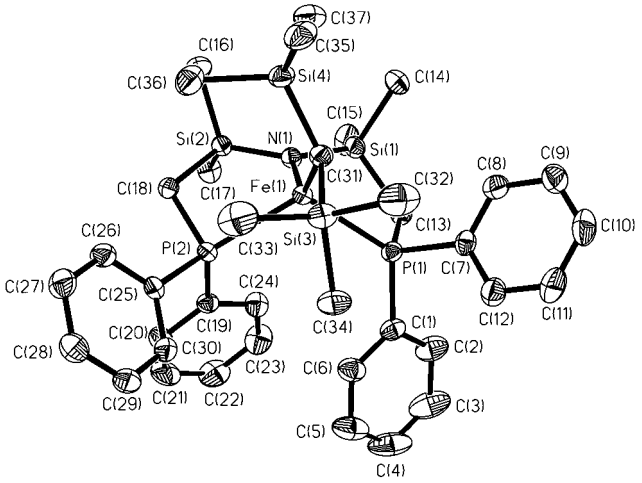

Figure 3. Molecular structure (ORTEP) and numbering scheme for $Fe\{CH(SiMe_3)_2\}[N(SiMe_2CH_2PPh_2)_2]$ (**6**), 33% probability ellipsoids are shown.

Table 4. Selected Bond Lengths (Å) and Angles (deg) in $Fe\{CH(SiMe_3)_2\}[N(SiMe_2CH_2PPh_2)_2]$ (6)

Fe(1)−P(1)	2.4886(6)	Fe(1)−P(2)	2.4924(6)
Fe(1)−N(1)	2.002(2)	Fe(1)−C(31)	2.069(2)
N(1)−Si(1)	1.710(2)	N(1)−Si(2)	1.713(2)
C(31)−Si(3)	1.856(2)	C(31)−Si(4)	1.857(2)
P(1)−Fe(1)−P(2)	110.39(2)	P(1)−Fe(1)−N(1)	92.78(5)
P(1)−Fe(1)−C(31)	109.65(6)	P(2)−Fe(1)−N(1)	87.03(5)
P(2)−Fe(1)−C(31)	121.39(6)	N(1)−Fe(1)−C(31)	131.20(7)
Fe(1)−P(1)−C(13)	99.32(7)	Fe(1)−P(2)−C(18)	94.76(7)
Fe(1)−N(1)−Si(1)	112.64(8)	Fe(1)−N(1)−Si(2)	117.36(8)
Si(1)−N(1)−Si(2)	129.93(10)	Fe(1)−C(31)−Si(3)	114.03(10)
Fe(1)−C(31)−Si(4)	116.73(10)	Si(3)−C(31)−Si(4)	115.96(11)

$-SiMe_3$), and loss of the entire alkyl group at 584 *m/e* ($M^+ - CH(SiMe_3)_2$).

The ^1H NMR spectra of these iron(II) alkyls are difficult to assign due to extreme broadness and missing peaks. The spectrum of the (trimethylsilyl)methyl complex **5** has two observable peaks at 11.6 and 0.0 ppm in a 2:1 integration, while the bis(trimethylsilyl)methyl complex **6** shows three peaks at 18.0, 13.4, and −4.2 ppm. Obviously there are many peaks absent from these spectra, precluding any assignment. However, these spectra can be used as fingerprints for the alkyl complexes.

The (trimethylsilyl)methyl complex **5**, while isolable for elemental analysis purposes, did not produce suitable crystals for X-ray diffraction, and moreover, it was found that complex **5** slowly decomposed over 1 week to the aforementioned brown material if left at room temperature. Fortunately, however, the very bulky bis(trimethylsilyl)methyl complex **6** is not only stable over months at room temperature but also can be obtained in crystalline form.

The structure is shown in Figure 3 and confirms the tetrahedral geometry around the iron(II) center and also the presence of the Fe−C bond. Selected bond lengths and angles are shown in Table 4. There is some distortion from pure tetrahedral; the coordination-sphere bond angles (ideally 109.5°) range from 87.03(5)° (N−Fe−P(2)) to 131.20(7)° (N−Fe−C(31)). This distortion is less than in the sterically crowded bis(ligand) complex **3**. The Fe−P bond lengths in alkyl **6** of 2.4886(6) and 2.4924(6) Å are very similar to those observed in the bis(ligand) complex **3** and to those observed in other high-spin tetrahedral iron(II) complexes. Similarly, the Fe−N bond length of 2.002(2) Å and the N−Si bond lengths of 1.710(2) and 1.713(2) Å are comparable to those observed in complex **3**.

A series of alkyls stabilized by 1,2-bis(diisopropylphosphino)ethane (dippe) has been prepared and the *p*-methylbenzyl complex $Fe(CH_2C_6H_4Me)_2$(dippe) structurally characterized with the Fe−C bond length measured to be 2.120(6) Å.[32] An alkyl−pyridine chelating ligand was used to prepare FeR_2 ($R = C(SiMe_3)_2C_5H_4N$-2), with Fe−C bond lengths of 2.154(8) and 2.139(7) Å.[33,34,39] In the case of **6**, the Fe−C(31) bond length of 2.069(2) Å is substantially shorter than the other iron(II) alkyls, despite the apparent steric bulk of the alkyl ligand. In fact, this bond length is shorter than that observed in $FeN_4(CO)(CH_3)$ (N_4 = macrocyclic tetradentate N-donor, $C_{10}H_{19}N_8$), an 18-electron macrocyclic complex with a terminal Fe−CH_3 ligand (2.077(5) Å).[40] The effect of the spin state on the Fe−C bond length in these complexes is unclear; there are not enough high-spin iron(II) alkyl complexes structurally characterized to address this point clearly.

Synthesis, Characterization, and Magnetic Properties of Iron(III) Dihalide Complexes. Upon addition of an excess of benzyl bromide to a toluene solution of the chloride **1** or bromide **2**, the solution slowly darkened to red-purple with the concomitant formation of a beige precipitate. X-ray-quality crystals of the beige precipitate could not be obtained, and thus this product was not unambiguously identified. From the above dark red toluene solution, we were able to isolate a complex that was identified as $FeBr_2[N(SiMe_2CH_2PPh_2)_2]$ (**7**) in moderate yield. This same product could also be made more rationally by dropwise addition of $LiN(SiMe_2CH_2PPh_2)_2$ to an ether solution of $FeBr_3$. Hence, the reaction could be generalized to produce the iron(III) dihalide complexes $FeX_2[N(SiMe_2CH_2PPh_2)_2]$ (X = Br (**7**), Cl (**8**)) (eq 7).

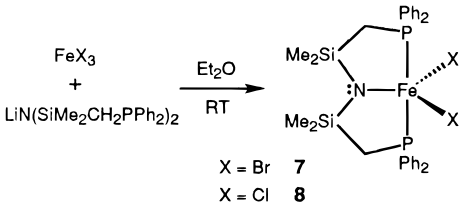

(7)

The solution magnetic moments of the dibromide **7** and dichloride **8** were measured to be 4.6 and 5.0 μ_B, respectively, by Evans' method.[10,11] These magnetic moments are obviously not indicative of high-spin $S = {}^5/_2$ centers (expected spin only magnetic moment, $\mu_{eff} = 5.92\ \mu_B$) but are also really too high to be considered as pure $S = {}^3/_2$ intermediate spin systems, even with the effects of spin−orbit coupling. Spin−orbit coupling in these systems would have to be second-order since the ground state is orbitally nondegenerate ($^4A_2$), so the effect should be relatively small. To compare, a true $S = {}^3/_2$ system for Fe(III) is exemplified by the bis(*N*,*N*-diethyldithiocarbamato)Fe(III)X (X = halide) series of

(39) Hursthouse, M. B.; Izod, K. J.; Motevalli, M.; Thornton, P. *Polyhedron* **1996**, *15*, 135.
(40) Goedken, V. L.; Peng, S. M. *J. Am. Chem. Soc.* **1974**, *96*, 7826.

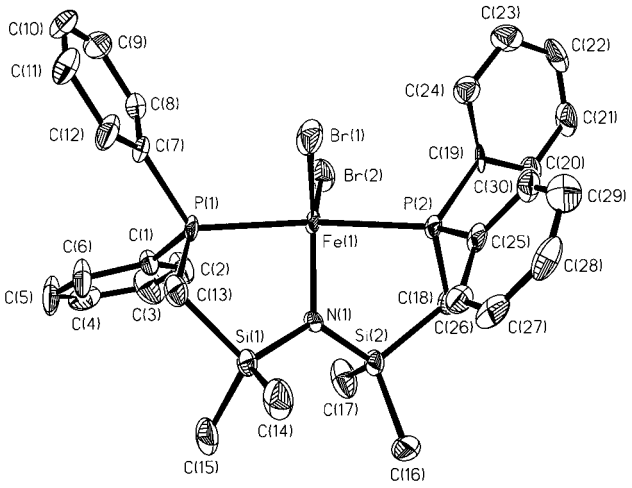

Figure 4. Molecular structure (ORTEP) and numbering scheme for $FeBr_2[N(SiMe_2CH_2PPh_2)_2]$ (**7**), 33% probability ellipsoids are shown.

Table 5. Selected Bond Lengths (Å) and Angles (deg) in $FeBr_2[N(SiMe_2CH_2PPh_2)_2]$ (7)

Fe(1)−P(1)	2.350(2)	Fe(1)−P(2)	2.330(2)
Fe(1)−N(1)	1.951(6)	Fe(1)−Br(1)	2.4201(13)
Fe(1)−Br(2)	2.4263(12)	N(1)−Si(1)	1.735(6)
N(1)−Si(2)	1.743(6)		
P(1)−Fe(1)−P(2)	173.35(8)	P(1)−Fe(1)−N(1)	87.3(2)
P(1)−Fe(1)−Br(1)	88.88(6)	P(2)−Fe(1)−N(1)	86.9(2)
P(2)−Fe(1)−Br(1)	91.66(6)	N(1)−Fe(1)−Br(1)	122.8(2)
P(1)−Fe(1)−Br(2)	97.60(6)	P(2)−Fe(1)−Br(2)	88.12(6)
Br(1)−Fe(1)−Br(2)	116.10(5)	N(1)−Fe(1)−Br(2)	121.0(2)
Fe(1)−P(1)−C(13)	99.4(3)	Fe(1)−P(2)−C(18)	103.0(2)
Fe(1)−N(1)−Si(1)	118.2(3)	Fe(1)−N(1)−Si(2)	116.1(3)
Si(1)−N(1)−Si(2)	125.5(3)		

complexes.[41−46] These distorted square-pyramidal complexes have room-temperature magnetic moments ranging from 3.92 to 4.07 μ_B depending on the halide, values which are quite close to the spin-only $S = {}^3/_2$ value of 3.87 μ_B.[42,45] An unusual, distorted iron(III) porphyrin, with a vinylidene group inserted into an Fe−N bond, has also been reported to be an intermediate-spin complex, with $\mu_{eff} = 3.9\ \mu_B$.[47] These values are found to be essentially temperature-independent (Curie law) except at very low temperatures where zero-field splitting causes a reduction in the observed moment.[46]

The X-ray structure of **7** is shown in Figure 4 and reveals a nearly perfect mononuclear, trigonal-bipyramidal arrangement of ligands around the iron center. Selected bond lengths and angles are given in Table 5. The axial P(1)−Fe−P(2) angle of 173.35(8)° and the equatorial angles of 122.8(2)°, 121.0(2)°, and 116.10(5)° for N−Fe−Br(1), N−Fe−Br(2), and Br(1)−Fe-Br(2), respectively indicate the minimal distortion around the iron center. The Fe−N bond of 1.951(6) Å in dibromide **7** is quite long compared to 1.918(4) Å in $Fe[N(SiMe_3)_2]_3$[48] and 1.896(5) and 1.900(5) Å in $FeI(py\text{-}d_5)(NRAr_f)_2$ ($R = C(CD_3)_2CH_3$; $Ar_f = 2,5\text{-}C_6H_3FMe$).[19] The N−Si bond lengths in **7** are 1.735(6) and 1.743(6) Å.

Other structurally characterized trigonal-bipyramidal iron(III) compounds include the pentaazidoiron(III) anion $Fe(N_3)_5^{2-}$,[49] $FeCl_3$(4-cyanopyridine)$_2$,[50] and $FeCl_3(NMe_3)_2$.[51] More recent and more relevant is the investigation by Walker and Poli of phosphine adducts of $FeCl_3$ and the influence of the phosphine on the spin state.[52] Two adducts were structurally characterized, namely $FeCl_3(PPh_3)_2$ and $FeCl_3(PMe_3)_2$, both of which are trigonal bipyramidal. The PPh_3 adduct as well as the earlier examples mentioned are all high-spin d^5 compounds with magnetic moments around 5.9 μ_B. The trimethylphosphine adduct was described as an "intermediate-spin" system ($S = {}^3/_2$; expected spin-only magnetic moment, $\mu_{eff} = 3.87\ \mu_B$)[9,12] on the basis of spectroscopic and magnetic data; it showed variable-temperature magnetic data with a value of 4.9 μ_B at room temperature, dropping to 4.2 μ_B at −78 °C. The Fe−P bond lengths in the high- and intermediate-spin systems are substantially different. In high-spin $FeCl_3(PPh_3)_2$, very long Fe−P distances of 2.654(4) and 2.623(4) Å are observed. In contrast, the Fe−P bonds in intermediate-spin $FeCl_3(PMe_3)_2$ are markedly shorter, at 2.342(5) and 2.332(5) Å. The Fe−P bonds in dibromide **7** are 2.330-(2) and 2.350(2) Å, which is consistent with the spin state of the iron(III) center having an $S = {}^3/_2$, intermediate-spin component.

Additional evidence for the presence of an $S = {}^3/_2$ component at the iron center is the UV−vis spectrum of the dihalide complexes. A pure $S = {}^5/_2$ spin metal complex, containing five unpaired electrons, would have no observable d−d transitions due to the lack of any spin-allowed transitions from a ground-state sextet term ($^6A_1$). However, an $S = {}^3/_2$ state will have spin-allowed transitions available for d−d transitions to be observed. Hence, while the detailed assignment of such bands is not vital, their observation signals the presence of an intermediate-spin Fe(III) center. Accordingly, the UV−vis spectra of dibromide **7** and dichloride **8** indicate that along with high-energy (>350 nm) charge-transfer bands, the visible region also contains spectral features that could be attributed to d−d transitions. The dibromide **7** has a dominating peak at 528 ($\epsilon = 5350\ M^{-1}\ cm^{-1}$) nm, a weaker band at 716 ($\epsilon = 1270\ M^{-1}\ cm^{-1}$) nm, and shoulders at 440 ($\epsilon = 3560\ M^{-1}\ cm^{-1}$) and 380 (4980 $M^{-1}\ cm^{-1}$) nm. The dichloride **8** has peaks at 330 ($\epsilon = 5990\ M^{-1}\ cm^{-1}$), 424 ($\epsilon = 6700\ M^{-1}\ cm^{-1}$) and 646 ($\epsilon = 1220\ M^{-1}\ cm^{-1}$) nm. The complex $FeCl_3(PMe_3)_2$ has a band at 378 ($\epsilon = 3400\ M^{-1}\ cm^{-1}$), 500 ($\epsilon = 10000\ M^{-1}\ cm^{-1}$), and 578 ($\epsilon = 2800\ M^{-1}\ cm^{-1}$) nm, while the high-spin $FeCl_3(PPh_3)_2$ has no spectral features below 360 nm.[52] These bands could be assigned to d−d transitions despite their large extinction coefficients as the Laporte selection rule is relaxed for five-coordinate

(41) Wickman, H. H.; Trozzolo, A. M.; Williams, H. J.; Hull, G. W.; Merritt, F. R. *Phys. Rev.* **1967**, *155*, 563.
(42) Martin, R. L.; White, A. H. *Inorg. Chem.* **1967**, *6*, 712.
(43) Hoskins, B. F.; White, A. H. *J. Chem. Soc. A* **1970**, 1668.
(44) Healy, P. C.; White, A. H.; Hoskins, B. F. *J. Chem. Soc., Dalton Trans.* **1972**, 1369.
(45) Chapps, G. E.; McCann, S. W.; Wickman, H. H.; Sherwood, R. C. *J. Chem. Phys.* **1974**, *60*, 990.
(46) Ganguli, P.; Marathe, V. R.; Mitra, S.; Martin, R. L. *Chem. Phys. Lett.* **1974**, *26*, 529.
(47) Mansuy, D.; Morgenstern-Badarau, I.; Lange, M.; Gans, P. *Inorg. Chem.* **1982**, *21*, 1427.
(48) Bradley, D. C.; Hursthouse, M. B.; Rodesiler, P. F. *J. Chem. Soc. D* **1969**, 14.
(49) Drummond, J.; Wood, J. S. *J. Chem. Soc., Chem. Commun.* **1969**, 1373.
(50) Daran, J. C.; Jeannin, Y.; Martin, L. M. *Inorg. Chem.* **1980**, *19*, 2935.
(51) Millington, K. R.; Wade, S. R.; Willey, G. R.; Drew, M. G. B. *Inorg. Chim. Acta* **1984**, *89*, 185.
(52) Walker, J. D.; Poli, R. *Inorg. Chem.* **1989**, *28*, 1793.

complexes, allowing for greater intensities than in octahedral systems. On the other hand, consideration of these absorbances as halide to metal charge-transfer bands, comparable to that observed in $CoX_2[N(SiMe_2CH_2PPh_2)_2]$ (X = Cl, Br), cannot be ruled out.[7]

The ^{1}H NMR spectra of the dihalide complexes featured broad peaks which were in some cases difficult to integrate. For the dichloride **8**, two equal intensity peaks at 25.9 and 22.5 ppm and a peak at −7.6 ppm of one-half the intensity were observed. A very broad peak could also be observed centered around 4 ppm. A variable temperature NMR study showed all peaks sharpening and shifting toward the diamagnetic range, as expected, but even at 60 °C assignments could not be made. The dibromide **7**, surprisingly, had a substantially different spectrum, with four observable peaks. Broad peaks at 6.9 and 9.0 ppm and a sharper peak at 10.1 ppm integrated 2:2:1 in intensity. There was also a very broad peak centered around 18 ppm, although the integration was difficult to obtain accurately. Most interesting, however, is the variable-temperature behavior of the dibromide **7**. Although the resonances due to the dichloride sharpen with increasing temperature, as normally expected, the resonances in the dibromide become broader and more paramagnetically shifted as the temperature is increased. A measurement of the magnetic susceptibility at increasing temperature confirmed this: the observed moment is $\mu_{eff} = 4.62\ \mu_B$ at 25 °C, 4.68 μ_B at 40 °C, and 4.75 μ_B at 60 °C. Both **7** and **8** are EPR silent in toluene solution and frozen glass, as observed for $FeCl_3(PMe_3)_2$.[52]

There are several possible explanations for the observed magnetic behavior of the dihalide compounds $FeX_2[N(SiMe_2CH_2PPh_2)_2]$ (X = Br (**7**), Cl (**8**)). The crystal structure showing a monomeric system rules out any iron−iron exchange interactions, so antiferromagnetic coupling of two high-spin $S = {}^5/_2$ centers can be discounted. Restricting the discussion to mononuclear systems, there are essentially three situations to consider. First, the assignment of the iron center as a pure intermediate-spin $S = {}^3/_2$ center with some orbital contribution to the moment can be considered and rejected, as the values of the room-temperature moments of **7** and **8** are really too high when compared to validated $S = {}^3/_2$ compounds. To obtain a higher moment, some high-spin $S = {}^5/_2$ character must be included into the complex. One possibility is that the room-temperature moment is fortuitously in the middle of a thermal equilibrium curve describing an $S = {}^3/_2$ (or even $S = {}^1/_2$) to $S = {}^5/_2$ spin transition. The low-high spin-equilibrium case is well-documented in the literature,[9,12] but there are only a few examples of spin equilibrium between $S = {}^3/_2$ and $S = {}^5/_2$ Fe(III).[9] One of these is the aforementioned $FeCl_3(PMe_3)_2$ which has variable-temperature magnetic data consistent with a thermal equilibrium between a ground-state $S = {}^3/_2$ center and low-lying $S = {}^5/_2$ center. Interestingly, changing the phosphine from PMe_3 to P(cyclohexyl)$_3$ yields another thermal equilibrium, this time with the $S = {}^5/_2$ state being the ground state.[52] The key feature of such an equilibrium is a large temperature dependence of the magnetic moment and a sigmoidal-type curve of the moment vs temperature. Finally, instead of observing a spin equilibrium between the $S = {}^3/_2$ and ${}^5/_2$ states, a quantum mechanical mixing of the two states can occur to create a new, discrete *spin-admixed* ground state that is neither $S = {}^3/_2$ nor ${}^5/_2$ but has elements of both.[9,53−56] Such admixed states give rise to magnetic properties that lie between the extremes of intermediate- and high-spin systems (i.e., $\mu_{eff} = 3.9-5.9\ \mu_B$).[47,55,57] Fe(TPP)$ClO_4$,[56,58] Fe(OEP)$ClO_4$,[56,59,60] and Fe(Pc)Cl[61] are the classic examples of complexes exhibiting this spin-admixed behavior, with room-temperature magnetic moments of 5.2, 4.8, and 4.53 μ_B, respectively, indicating different amounts of spin-state mixing depending on the ligand set. In addition, the temperature dependence of such a spin-admixed system is quite different than that of spin-crossover complexes. Instead of a sigmoidal curve, essentially Curie-law behavior with a slight reduction in moment over a large temperature range is observed.[53,56,58,61] At low temperatures, other factors such as zero-field splitting begin to become important and the moment often decreases faster. However, no sharp transition is observed. Hence, it should be possible to differentiate spin-admixed systems from spin-crossover systems on the basis of a variable-temperature magnetics study.

A solid-state variable-temperature magnetic susceptibility study of dibromide **7** using a SQUID magnetometer revealed a slow, smooth reduction in moment from 4.70 μ_B at 300 K to 4.45 μ_B at 20 K and not a sharp, spin-crossover curve (Figure 5). That is, the magnetic moment more or less obeyed the Curie law over the temperature range discussed. From 20 K, the moment begins to drop more rapidly; at 2 K, the observed magnetic moment is 3.49 μ_B. Hence, it appears that dibromide **7** is a rare example of a spin-admixed Fe(III) system and is to our knowledge the first documented trigonal-bipyramidal spin-admixed Fe(III) complex.

Conclusions

In this work, the coordination chemistry of the tridentate mixed-donor ligand $N(SiMe_2CH_2PPh_2)_2$ has been investigated with iron in both the divalent and trivalent formal oxidation states. As expected, the divalent halide complexes $FeX[N(SiMe_2CH_2PPh_2)_2]$ are d^6, high-spin, tetrahedral systems. These complexes can be functionalized to generate the corresponding hydrocarbyl derivatives $FeR[N(SiMe_2CH_2PPh_2)_2]$ as long as the alkyl ligand R is bulky; for example, the methyl derivative and the benzyl complex could not be isolated at room temperature as decomposition was observed. However, for R = CH_2SiMe_3 and $CH(SiMe_3)_2$, isolable complexes were formed. These alkyl derivatives also

(53) Maltempo, M. M. *J. Chem. Phys.* **1974**, *61*, 2540.
(54) Bominaar, E. L.; Block, R. *J. Chem. Phys.* **1991**, *95*, 6712.
(55) Reed, C. A.; Guiset, F. *J. Am. Chem. Soc.* **1996**, *118*, 3281.
(56) Mitra, S.; Marathe, V. R.; Birdy, R. *Chem. Phys. Lett.* **1983**, *96*, 103.
(57) Cheng, R.-J.; Chen, P.-Y.; Gau, P.-R.; Chen, C.-C.; Peng, S.-M. *J. Am. Chem. Soc.* **1997**, *119*, 2563.
(58) Reed, C. A.; Mashiko, T.; Bentley, S. P.; Kastner, M. E.; Scheidt, W. R.; Spartalian, K.; Lang, G. *J. Am. Chem. Soc.* **1979**, *101*, 2948.
(59) Ogoshi, H.; Sugimoto, H.; Watanabe, E.-I.; Yoshida, Z.-I.; Maeda, Y.; Sakai, H. *Bull. Chem. Soc. Jpn.* **1981**, *54*, 3414.
(60) Masuda, H.; Taka, T.; Osaki, K.; Sugimoto, H.; Yoshida, Z.-I.; Ogoshi, H. *Inorg. Chem.* **1980**, *19*, 950.
(61) Kennedy, B. J.; Murray, K. S.; Zwack, P. R.; Homborg, H.; Kalz, W. *Inorg. Chem.* **1986**, *25*, 2539.

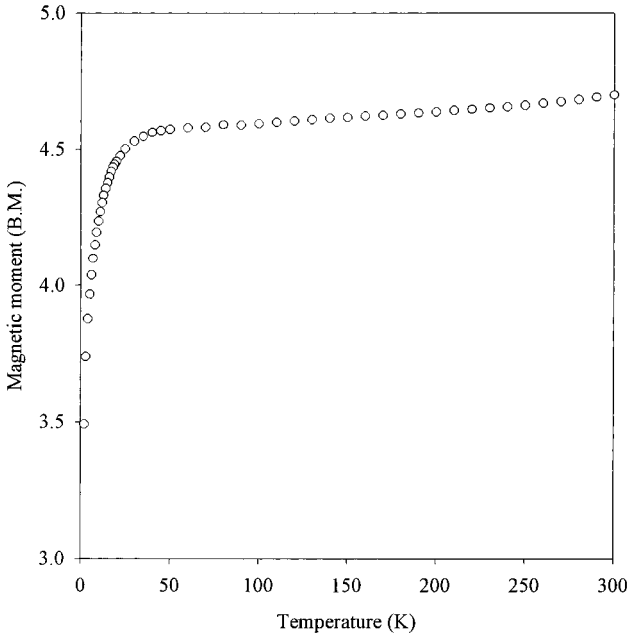

Figure 5. Graph of magnetic moment vs temperature for $FeBr_2[N(SiMe_2CH_2PPh_2)_2]$ (7).

have high-spin, tetrahedral geometries. When the halide is replaced by a cyclopentadienyl ligand, a pseudotetrahedral structure for $Fe(\eta^5\text{-}C_5H_5)[N(SiMe_2CH_2PPh_2)_2]$ is obtained and it is found that the complex is diamagnetic; this formally 18-electron species is, thus, an analogue of ferrocene.

The corresponing trivalent iron complexes $FeX_2[N(SiMe_2CH_2PPh_2)_2]$ (X = Br, Cl) could be obtained directly by reaction of $LiN(SiMe_2CH_2PPh_2)_2$ with $FeBr_3$ or $FeCl_3$, respectively. The X-ray structure of dibromide $FeBr_2[N(SiMe_2CH_2PPh_2)_2]$ shows it to have a nearly perfect trigonal-bipyramidal geometry. The magnetic susceptibility of the dibromide is characteristic of a spin-admixed system, a particularly rare type of magnetic behavior.

Experimental Section

General Procedures. Unless otherwise stated, all manipulations were performed under an atmosphere of dry, oxygen-free dinitrogen or argon by means of standard Schlenk or glovebox techniques. The glovebox used was a Vacuum Atmospheres HE-553-2 workstation equipped with a MO-40-2H purification system and a −40 °C freezer. ^1H NMR spectroscopy was performed at room temperature on a Bruker WC-400 or a Bruker AC-200 instrument operating at 400 or 200 MHz, respectively, and referenced to internal C_6D_5H (7.15 ppm). $^{31}P\{^1H\}$ NMR spectroscopy was performed on a Varian XL-300 instrument operating at 121.4 MHz and referenced to external $P(OMe)_3$. Magnetic moments were measured by a modification of Evans' method[10,11] (C_6D_5H or Cp_2Fe as a reference peak) on the NMR spectrometers listed above. The variable-temperature magnetic susceptibility of a powdered sample of dibromide **7** was measured over the range 2−300 K and at a field of 10 000 G using a Quantum Design (MPMS) SQUID magnetometer. The sample holder, made from PVC, was specially designed to possess a constant cross-sectional area. Infrared spectra were recorded on a BOMEM MB-100 spectrometer. UV−vis spectra were recorded on a HP-8452A or HP-8453A diode array spectrophotometer. Mass spectra were measured using a Kratos MS-50 EI instrument operating at 70 eV. Microanalyses (C, H, N) were performed by Mr. P. Borda of this department.

The alkali-metal salts $LiN(SiMe_2CH_2PPh_2)_2$,[62] $LiCH(SiMe_3)_2$,[63] and KCH_2Ph[64] were prepared by the methods described in the literature. $FeCl_2$, $FeBr_2$, and $FeBr_3$ were either used as received or dried in refluxing Me_3SiCl. $FeCl_3$ (99.99%, Aldrich) was used as received. Benzyl bromide and benzyl chloride were dried by being eluted through a column of activated alumina and then degassed by three freeze−pump−thaw cycles. NaCp·DME was prepared by the reaction of Na with CpH in dry DME. All other reagents were obtained from commercial sources and used as received.

Hexanes, toluene, and THF were heated to reflux over CaH_2 prior to a final distillation from either sodium metal or sodium benzophenone ketyl under an Ar atmosphere. Deuterated solvents were dried by activated 3-Å molecular sieves; oxygen was removed by trap-to-trap distillation and three freeze−pump−thaw cycles.

Synthesis of $FeCl[N(SiMe_2CH_2PPh_2)_2]$ (1). A solution of $LiN(SiMe_2CH_2PPh_2)_2$ (2.5 g, 4.7 mmol) in 30 mL of THF was added dropwise to anhydrous $FeCl_2$ (0.65 g, 5.15 mmol) suspended in 20 mL of THF at room temperature. The suspended iron chloride slowly dissolved to give a brown solution, which was stirred for 5 h. The solvent was then removed in vacuo, and the residue was extracted with toluene and filtered through Celite to give a light brown solution. The toluene solution was reduced to a minimum amount and placed overnight in a −40 °C freezer, after which $FeCl[N(SiMe_2CH_2PPh_2)_2]$ (**1**) was isolated as a beige powder. Yield: 2.3 g (79%). Anal. Calcd for $C_{30}H_{36}ClFeNP_2Si_2\cdot 0.5C_7H_8$: C, 60.40; H, 5.85; N, 2.26. Found: C, 60.34; H, 6.15; N, 2.31. ^1H NMR (C_6D_6): δ 16.5 (v br, 12H), 13.3 (br, 8H), −1.8 (s, 4H) and resonances integrating correctly for 0.5 C_7H_8. MS: *m/e* 619 (M^+), 584 ($M^+ - Cl$). $\mu_{eff} = 4.9\ \mu_B$.

Synthesis of $FeBr[N(SiMe_2CH_2PPh_2)_2]$ (2). The reaction was performed as for the preparation of **1**, using $FeBr_2$ (0.10 g, 0.46 mmol) as the starting material. After workup, $FeBr[N(SiMe_2CH_2PPh_2)_2]$ (**2**) was isolated as a beige powder. Yield: 0.20 g (72%). Anal. Calcd for $C_{30}H_{36}BrFeNP_2Si_2\cdot 0.5C_7H_8$: C, 56.63; H, 5.67; N, 1.97. Found: C, 56.84; H, 5.67; N, 2.30. MS: *m/e* 665 (M^+), 584 ($M^+ - Br$). $\mu_{eff} = 5.0\ \mu_B$.

Reaction of $FeCl[N(SiMe_2CH_2PPh_2)_2]$ (1) with pyridine. Addition of a 20% excess of pyridine to a 5-mL THF solution of $FeCl[N(SiMe_2CH_2PPh_2)_2]$ (**1**) (0.05 g, 0.08 mmol) caused an immediate coloration of the solution to a dark yellow-orange. After 30 min, the solvents were removed in vacuo and the product extracted with hexanes. An impure yellow solid which analyzed for **1**·(2 − *x*)py (*x* corresponds to loss of pyridine from the halide complex) was obtained upon slow evaporation of hexanes; the pyridine adduct cannot be isolated as a solid. μ_{eff} (**1** in C_5D_5N) = $4.9\ \mu_B$.

Synthesis of $Fe[N(SiMe_2CH_2PPh_2)_2]_2$ (3). Method 1. To a pale yellow 10-mL toluene solution of $FeCl[N(SiMe_2CH_2PPh_2)_2]$ (**1**) (0.050 g, 0.081 mmol) was added a 10-mL toluene solution of $LiN(SiMe_2CH_2PPh_2)_2$ (0.043 g, 0.081 mmol) dropwise. No color change occurred, and after being stirred overnight, the toluene was removed in vacuo and the residue extracted with hexanes and filtered through Celite to yield a pale yellow solution. Slow evaporation of the hexanes solution over 2 days yielded large, very pale green crystals of $Fe[N(SiMe_2CH_2PPh_2)_2]_2$ (**3**) from which the X-ray crystal structure was obtained.

Method 2. To a suspension of $FeCl_2$ (0.018 g, 0.14 mmol) in 10 mL of THF was added $LiN(SiMe_2CH_2PPh_2)_2$ (0.15 g, 0.28 mmol) in 10 mL of THF dropwise. The iron chloride was slowly dissolved to give a pale brown-yellow solution, which

(62) Fryzuk, M. D.; MacNeil, P. A.; Rettig, S. J.; Secco, A. S.; Trotter, J. *Organometallics* **1982**, *1*, 918.
(63) Cowley, A. H.; Kemp, R. A. *Synth. React. Inorg. Met.-Org. Chem.* **1981**, *11*, 591.
(64) Schlosser, M.; Ladenberger, V. *J. Organomet. Chem.* **1967**, *8*, 193.

became pale yellow-green overnight. The THF was removed in vacuo, and the residue was extracted with hexanes and filtered through Celite to give a pale yellow-green solution from which pale green crystals of $Fe[N(SiMe_2CH_2PPh_2)_2]_2$ (**3**) were deposited. Yield: 0.13 g (84%). Anal. Calcd for $C_{60}H_{72}FeN_2P_4Si_4$: C, 64.73; H, 6.52; N, 2.52. Found: C, 64.73; H, 6.69; N, 2.42. ^{1}H NMR (C_6D_6): δ 20.5 (v br, 12H, Si*Me*$_2$), 10.8 (br, 8H, *m*-Ph), 1.0 (v br, 8H, *o*-Ph), −1.0 (br, 4H, *p*-Ph). MS: *m/e* 1112 (M^+), 1097 ($M^+ - CH_3$), 913 ($M^+ - CH_2PPh_2$), 584 ($M^+ - N(SiMe_2CH_2PPh_2)$). $\mu_{eff} = 4.7\ \mu_B$.

Attempted Synthesis of FeMe[N(SiMe$_2$CH$_2$PPh$_2$)$_2$]. To a 20-mL THF solution of $FeCl[N(SiMe_2CH_2PPh_2)_2]$ (**1**) (0.20 g, 0.32 mmol) at −78 °C was added MeLi (0.47 M, 0.7 mL, 0.33 mmol) dissolved in 10 mL of THF dropwise. The pale yellow solution rapidly turned golden brown, and after being stirred for 15 min at −78 °C, it was warmed to room temperature. The solution darkened to a dark brown during 1 h of stirring. After removal of the solvent, an uncharacterizable dark brown residue was obtained. The reaction was repeated using MeMgBr (0.33 M, 0.73 mL, 0.24 mmol) and $FeCl[N(SiMe_2CH_2PPh_2)_2]$ (**1**) (0.15 g, 0.24 mmol), and in this case, a bright yellow solution was obtained at −78 °C. However, upon being warmed to room temperature, the same brown oil was isolated. Attempts to perform the metathesis by prior addition of pyridine resulted eventually in the formation of intractable brown oils.

Attempted Synthesis of Fe(CH$_2$Ph)[N(SiMe$_2$CH$_2$PPh$_2$)$_2$]. To a 20-mL THF solution of $FeCl[N(SiMe_2CH_2PPh_2)_2]$ (**1**) (0.15 g, 0.24 mmol) at −78 °C was added a 10-mL THF solution of KCH_2Ph (0.031 g, 0.24 mmol) dropwise. A bright yellow solution formed immediately, which persisted after 15 min of stirring at low temperature. Upon being warmed to room temperature, the solution remained yellow, but after 30 min of stirring at room temperature, the color darkened to a dark brown. Attempts to remove the solvent at low temperature to intercept the yellow compound resulted in the eventual isolation of intractable brown oils or solids. Addition of pyridine at low temperature caused a color change to red, but upon warming the same brown mixture was obtained.

Synthesis of Fe(η^5-C$_5$H$_5$)[N(SiMe$_2$CH$_2$PPh$_2$)$_2$] (4). To a 10-mL THF solution of $FeCl[N(SiMe_2CH_2PPh_2)_2]$ (**1**) (0.15 g, 0.24 mmol) at −78 °C was added a 10-mL THF solution of NaC_5H_5·DME (0.043 g, 0.24 mmol) dropwise to cause an immediate color change to deep red. The reaction mixture was warmed to room temperature and stirred for 30 min, after which the solvent was removed in vacuo, the residue extracted with hexanes and filtered through Celite, and the resulting red solution evaporated to yield deep red Fe(η^5-C_5H_5)[N(SiMe$_2$CH$_2$PPh$_2$)$_2$]·C_6H_{14} (**4**·C_6H_{14}). Yield: 0.13 g (82%). Anal. Calcd for $C_{35}H_{41}FeNP_2Si_2 \cdot C_6H_{14}$: C, 66.92; H, 7.20; N, 1.90. Found: C, 67.02; H, 7.20; N, 1.85. ^{1}H NMR (C_6D_6): δ 7.43 (m, 8H, *o*-Ph), 7.05 (m, 12H, *m*-, *p*-Ph), 3.95 (s, 5H, C_5H_5), 1.3 (m, 2H, C*H*H), 0.85 (m, 2H, CH*H*), 0.25 (s, 6H, Si*Me*$_2$), 0.00 (s, 6H, Si*Me*$_2$) and resonances integrating correctly for C_6H_{14}. ^{31}P-{^{1}H} NMR (C_6D_6): δ −22.5. UV−vis (C_7H_8): 494 nm. MS: *m/e* 649 (M^+), 584 ($M^+ - C_5H_5$). X-ray-quality crystals were obtained by slow evaporation of a hexanes solution of **4** to yield deep red prisms of Fe(η^5-C_5H_5)[N(SiMe$_2$CH$_2$PPh$_2$)$_2$] (**4**).

Synthesis of Fe(CH$_2$SiMe$_3$)[N(SiMe$_2$CH$_2$PPh$_2$)$_2$] (5). To a 10-mL THF solution of $FeCl[N(SiMe_2CH_2PPh_2)_2]$ (**1**) (0.057 g, 0.092 mmol) at −78 °C was added a 10-mL THF solution of $LiCH_2SiMe_3$ (0.009 g, 0.096 mmol) dropwise to yield a bright yellow solution. This was warmed to room temperature; the yellow color persisted after overnight stirring. The solvent was removed in vacuo, and the residue was extracted with hexanes, filtered through Celite, and concentrated. After overnight slow evaporation, crystals of $Fe(CH_2SiMe_3)[N(SiMe_2CH_2PPh_2)_2]$ (**5**) formed from the yellow solution. Yield: 0.051 g (86%). Anal. Calcd for $C_{34}H_{47}FeNP_2Si_3$: C, 60.79; H, 7.05; N, 2.08. Found: C, 61.12; H, 7.03; N, 2.04. ^{1}H NMR (C_6D_6): δ 11.6 (br, 2nH), 0.0 (br, *n*H). MS: *m/e* 584 ($M^+ - CH_2SiMe_3$). $\mu_{eff} = 4.8\ \mu_B$.

Synthesis of Fe{CH(SiMe$_3$)$_2$}[N(SiMe$_2$CH$_2$PPh$_2$)$_2$] (6). The reaction was performed in the same manner as for **5**, using 0.40 g (0.65 mmol) of $FeCl[N(SiMe_2CH_2PPh_2)_2]$ (**1**) and $LiCH(SiMe_3)_2$ (0.11 g, 0.65 mmol). Large pale yellow crystals of Fe{$CH(SiMe_3)_2$}[$N(SiMe_2CH_2PPh_2)_2$] (**6**), suitable for X-ray diffraction analysis, were deposited upon slow evaporation of the final hexanes solution. Yield: 0.33 g (69%). Anal. Calcd for $C_{37}H_{55}FeNP_2Si_4$: C, 59.73; H, 7.45; N, 1.88. Found: C, 60.10; H, 7.41; N, 1.86. ^{1}H NMR (C_6D_6): δ 18.0 (v br, 9H), 13.4 (br, 4H), −4.2 (v br). MS: *m/e* 743 (M^+), 742 ($M^+ - H$), 728 ($M^+ - CH_3$), 670 ($M^+ - SiMe_3$), 584 ($M^+ - CH(SiMe_3)_2$). $\mu_{eff} = 5.3\ \mu_B$.

Reaction of FeX[N(SiMe$_2$CH$_2$PPh$_2$)$_2$] (X = Cl, Br) with Benzyl Bromide. A 0.10 g amount of $FeX[N(SiMe_2CH_2PPh_2)_2]$ (X = Cl, 0.16 mmol; X = Br, 0.15 mmol) was dissolved in 10 mL of toluene to give a pale yellow solution. To this was added 0.3 mL (2.5 mmol) of neat benzyl bromide. No immediate reaction occurred, but a cherry red color slowly developed over 1 h and intensified overnight, with concurrent formation of a beige precipitate. After being stirred overnight, the toluene solution was decanted and filtered through Celite to give a red solution to which was added hexanes (0.5 mL). Long red bars of $FeBr_2[N(SiMe_2CH_2PPh_2)_2]$ (**7**) formed overnight from the red solution. Yield: 0.05 g (37% for X = Cl, 40% for X = Br). Anal. Calcd for $C_{30}H_{36}FeBr_2NP_2Si_2 \cdot C_7H_8$: C, 53.12; H, 5.30; N, 1.67. Found: C, 53.33; H, 5.37; N, 1.73. ^{1}H NMR (C_6D_6): δ 6.9 (br, 8H), 9.0 (br, 8H), 10.1 (s, 4H), 18 (v br) and resonances integrating correctly for C_7H_8. UV−vis (C_7H_8): 380 (ϵ = 4980 M^{-1} cm^{-1}), 440 (ϵ = 3560 M^{-1} cm^{-1}), 528 (ϵ = 5350 M^{-1} cm^{-1}), 700 (ϵ = 1270 M^{-1} cm^{-1}) nm. MS: *m/e* 663 (M^+ − Br), 464 (M^+ − Br − CH_2PPh_2). $\mu_{eff} = 4.6\ \mu_B$.

Synthesis of FeBr$_2$[N(SiMe$_2$CH$_2$PPh$_2$)$_2$] (7). Method 1. As described above, addition of benzyl bromide to $FeX[N(SiMe_2CH_2PPh_2)_2]$ (X = Cl, Br) gives $FeBr_2[N(SiMe_2CH_2PPh_2)_2]$ (**7**) in moderate yield.

Method 2. Anhydrous $FeBr_3$ (0.18 g, 0.61 mmol) was dissolved in 10 mL of diethyl ether to give a yellow-red solution. To this was added a 10-mL ether solution of $LiN(SiMe_2CH_2PPh_2)_2$ (0.30 g, 0.56 mmol) dropwise at room temperature to give an immediate color change to an intense inky purple-red. The reaction was stirred overnight, and the solvent was removed in vacuo. The residue was extracted with toluene and filtered through Celite, and hexanes were carefully added dropwise until precipitation began. The flask was capped, and dark red bars of $FeBr_2[N(SiMe_2CH_2PPh_2)_2] \cdot C_7H_8$ (**7**) were deposited overnight. Yield: 0.33 g (78%). Crystals suitable for X-ray diffraction were obtained by slow evaporation of a benzene solution of **7**.

Synthesis of FeCl$_2$[N(SiMe$_2$CH$_2$PPh$_2$)$_2$] (8). Anhydrous $FeCl_3$ (0.035 g, 0.21 mmol) was dissolved in 10 mL of diethyl ether to give a bright yellow solution. To this was added a 10-mL ether solution of $LiN(SiMe_2CH_2PPh_2)_2$ (0.10 g, 0.19 mmol) dropwise at room temperature to give an immediate color change to dark green-black. The reaction was stirred overnight, and then the solvent was removed in vacuo. The residue was extracted with toluene and filtered through Celite, hexanes were added (60:40 hexanes: toluene), and the solution was put into a −40 °C freezer. Black-green prisms of $FeCl_2[N(SiMe_2CH_2PPh_2)_2] \cdot C_7H_8$ (**8**) were deposited overnight. Yield: 0.11 g (90%). Anal. Calcd for $C_{30}H_{36}FeCl_2NP_2Si_2 \cdot C_7H_8$: C, 59.44; H, 5.93; N, 1.87. Found: C, 59.70; H, 5.85; N, 1.87. ^{1}H NMR (C_6D_6): δ 25.9 (br, 8H), 22.5 (v br, 8H), 4 (v br), −7.6 (br, 4H) and resonances integrating correctly for C_7H_8. UV−vis (C_7H_8): 330 (ϵ = 5990 M^{-1} cm^{-1}), 424 (ϵ = 6700 M^{-1} cm^{-1}), 646 (ϵ = 1220 M^{-1} cm^{-1}) nm. MS: *m/e* 654 (M^+), 619 (M^+ − Cl). $\mu_{eff} = 5.0\ \mu_B$.

Titration of FeCl[N(SiMe$_2$CH$_2$PPh$_2$)$_2$] (1) with Pyridine. The titration of $FeCl[N(SiMe_2CH_2PPh_2)_2]$ (**1**) with pyridine was monitored by UV−vis spectroscopy by monitoring the growth of a band at 370 nm and then at 388 nm. The titration was performed in an airtight quartz cell in which 0.01 g of chloride **1** was dissolved in 10 mL of toluene (1.6×10^{-3}

M). Pyridine was added by injection through a septum. For the first equilibrium, diluted pyridine was added (0.32 M in toluene, 0.02−0.05 mL per injection). Neat pyridine was used for the second equilibrium titration (0.02−0.05 mL per injection). After addition of about 10 equiv of pyridine, a band at 370 nm was observed. Addition of approximately 1000 equiv of pyridine resulted in a band at 388 nm. Equilibrium constants were calculated from the slopes of plots based on a crude estimate of the endpoint of the first titration according to the loss of an isosbestic point after a certain amount of pyridine was added. K_1 and K_2 may be estimated by plots of log [FeCl(py)[N($SiMe_2CH_2PPh_2$)$_2$]]/[FeCl[N($SiMe_2CH_2PPh_2$)$_2$]] versus log [pyridine] and log [FeCl(py)$_2$[N($SiMe_2CH_2PPh_2$)$_2$]]/[FeCl(py)[N($SiMe_2CH_2PPh_2$)$_2$]] versus log [pyridine], respectively.

The endpoint of the first equilibrium was assumed to be at the point where all of **1** had reacted to form **1**·py and no **1**·py$_2$ had yet formed, as illustrated by the subsequent loss of the isosbestic point as more pyridine was added. As increasing amounts of pyridine were added, the 370 nm charge-transfer band shifted to 388 nm. The endpoint to the second equilibrium was assumed to be at the point where no increase in absorbance to the 388 nm band was observed and that only **1**·py$_2$ existed in the solution.

X-ray Crystallographic Analyses of Fe[N($SiMe_2CH_2PPh_2$)$_2$]$_2$ (3), Fe(η^5-C_5H_5)[N($SiMe_2CH_2PPh_2$)$_2$] (4), Fe{CH($SiMe_3$)$_2$}[N($SiMe_2CH_2PPh_2$)$_2$] (6), and $FeBr_2$[N($SiMe_2CH_2PPh_2$)$_2$] (7). Suitable crystals of **3**, **6**, and **7** were attached to thin glass fibers with epoxy cement and mounted on the Siemens SMART system for a data collection at 173(2) K. Crystallographic data are summarized in Table 1. Unit-cell parameters were calculated either from 60 or 90 data frames collected at different sections of the Ewald sphere. The unit-cell parameters and the systematic absences in the diffraction data were uniquely consistent with the reported space groups. A semiempirical absorption correction was applied based on redundant data at varying effective azimuthal angles.

The structures were solved by direct methods, completed by subsequent Fourier synthesis, and refined with full-matrix least-squares methods. All non-hydrogen atoms were refined with anisotropic displacement coefficients. All hydrogen atoms were treated as idealized contributions. Scattering factors and anomalous dispersion coefficients are contained in the SHELXTL 5.03 program library.[65]

Crystals of **4** were mounted in a capillary under N_2 and analyzed using a Rigaku AFC6S; crystallographic data appear in Table 1. The final unit-cell parameters were obtained by least-squares methods on the setting angles for 25 reflections with $2\theta = 23.9-31.4°$. The intensities of three standard reflections, measured every 200 reflections, showed only small random fluctuations. The data were processed[66] and corrected for Lorentz and polarization effects, and absorption (empirical, based on azimuthal scans).

The structure was solved by the Patterson method. All non-hydrogen atoms were refined with anisotropic thermal parameters. Hydrogen atoms were fixed in idealized positions (staggered methyl groups, C−H = 0.98 Å, $B_H = 1.2\ B_{\text{bonded atom}}$). No correction for secondary extinction was necessary. Neutral atom scattering factors and anomalous dispersion corrections were taken from the *International Tables for X-ray Crystallography*.[67]

Selected bond lengths and angles appear in Tables 2−5. Final atomic coordinates and equivalent isotropic thermal parameters, complete tables of bond lengths and angles, hydrogen atom parameters, anisotropic thermal parameters, torsion angles, intermolecular contacts, and least-squares planes are included as Supporting Information.

Acknowledgment. Professor R. C. Thompson and Mr. D. Summers are thanked for help in the measurement of the magnetic susceptibility of the iron(III) dibromide **7**. Financial support was obtained from NSERC in the form of a 1967 Science and Engineering Postgraduate Scholarship (D.B.L.) and a Research grant (M.D.F.).

Supporting Information Available: For **3**, **4**, **6**, and **7**, complete crystallographic data, atomic coordinates and equivalent isotropic thermal parameters, anisotropic thermal parameters and complete listings of bond lengths and angles, torsion angles, intermolecular contacts, and least-squares planes for **4** (45 pages). Ordering information is given on any masthead page.

OM970665I

(65) *SHELXTL-Plus V5.0*; Siemens Industrial Automation, Inc.: Madison, WI.

(66) *teXsan*: *Crystal Structure Analysis Package*; Molecular Structure Corp.: The Woodlands, TX, 1995.

(67) (a) *International Tables for X-ray Crystallography*; Kynoch Press: Birmingham, U.K. (present distributor Kluwer Academic Publishers: Boston, MA), 1974; Vol. IV, pp 99−102. (b) *International Tables for Crystallography*; Kluwer Academic Publishers: Boston, MA, 1992; Vol. C, pp 200−206.